Air Sparging for Subsurface Remediation: Numerical Analysis Using T2VOC

John E. McCray
Department of Environmental Systems Engineering, Clemson University, Clemson, SC 29634-0919
Currently at Department of Hydrology and Water Resources, Harshbarger Building 11, University of Arizona, Tucson, AZ 85721

Ronald W. Falta
Department of Earth Sciences, Clemson University, Clemson, SC 29634-1908

Abstract. Air sparging is under active investigation as a promising remediation technology for aquifers contaminated with volatile organic dense nonaqueous phase liquids (DNAPLs). A theoretical study for the removal of DNAPLs from the subsurface using this technology is presented. T2VOC is used to conduct multiphase numerical simulations of DNAPL removal utilizing a model aquifer with a radially-symmetric geometry. Both homogeneous and macroscale heterogeneous systems are considered. These simulations suggest that DNAPLs are efficiently removed in a zone of contaminant cleanup at relatively low gas saturations within the injected air plume. The zone of effective removal may be referred to as the radius of influence (ROI). The sparging-induced pressure increase below the water table, which may be measured in the field, is recommended as the best method for determining the ROI. Multiphase numerical simulations are used to support this recommendation, to relate the injected gas ROI to the zone of NAPL cleanup, and to illustrate the transient and steady-state aquifer behavior.

Introduction

DNAPLs are an increasingly common subsurface pollution problem. DNAPLs, which are denser than water, may act as a long-term source of ground water contamination in the saturated zone due to typically low aqueous solubilities. Air sparging is an innovative ground water remediation technology which shows promise in removing DNAPLs from the subsurface. Air sparging works on the principles of interphase mass transfer. Air is injected into the saturated zone below a contaminated area. As the air rises to the surface, dissolved and NAPL contaminant will partition into the gas phase when in contact with the air. Air sparging is typically coupled with a soil vapor extraction (SVE) system to collect the volatilized pollutant in the vadose zone. In some cases, sparging may be less costly and more effective than conventional pump-and-treat (Felten et al., 1992; Leonard and Brown, 1992; Loden, 1992).

Perhaps the most important parameter in an air sparging system design is the radius of influence (ROI) of the sparging well. Four methods currently used to estimate the sparge well ROI are: measuring the pressure response below the water table, measuring the increase in dissolved oxygen concentration in the ground water, measuring the mounding of the water table, and measuring increases in VOC vapor concentration in the unsaturated zone (Felten et al., 1992; Leonard and Brown, 1992; Loden, 1992). It is not clear, however, which of these methods best define the ROI. Ideally, the ROI should correspond to contaminant cleanup. Based on our numerical analysis, we recommend measurement of the pressure increase (above hydrostatic) in the sparge zone, or "positive pressure" as the most accurate method for ROI estimation. The numerical simulations presented here will demonstrate the utility of the recommended method, as well as show how the sparging ROI is related to NAPL cleanup under certain conditions. The simulations will also illustrate the significance of macro-scale heterogeneities (such as clay lenses) on sparging effectiveness. The transient and steady-state development of the injected gas plumes in our model systems is also discussed.

Adenekan et al. (1990) used STMVOC (see Falta et al. 1992a) to compare the effectiveness of air sparging, vapor extraction, and groundwater extraction for DNAPL removal. We use T2VOC (Pruess, 1991) for a detailed three-phase numerical study focused on air sparging in hopes that our study will contribute to the limited theoretical knowledge on the subject. The code has been validated with experimental data for several multiphase transport problems (Falta et al, 1992b; Falta, 1990, Seely et al, 1994). Recently, McCray (1994) used T2VOC to successfully model the air sparging experiment of Ji et al. (1993). The laboratory experiment demonstrated that air injected into a saturated medium of glass beads formed stable, parabolic-shaped plumes at steady state. While these plumes actually consisted of many discrete air channels, the average behavior on a larger scale appeared to be a stable, multiphase flow process. T2VOC simulated the shape and multiphase behavior of various plumes quite well under different flow conditions in both homogeneous and heterogeneous media.

Physical System and Model Representation

The physical system considered is a 20 m deep sandy aquifer, bounded on the bottom by an impervious barrier. The water table exists 10 m below the ground surface. The capillary fringe is about 0.5 m thick. The heterogeneous case contains a 3.5 meter radius, low permeability, high capillary "clay" disk of thickness 1 m located at mid-depth in the saturated zone. The radially-symmetric model is shown in Figure 1. The arrangement of sparging and SVE well screens is nested as shown, which is common in actual remediation scenarios (Loden, 1992). TCE is used as the pollutant. Physical and chemical data used for TCE is the same as in Falta et al. (1992b).

The top of the model aquifer is a constant, atmospheric pressure boundary, while the bottom is a "no-flow" boundary. The outer boundary, which is beyond the zone affected by sparging, is a static pressure, static fluid saturation, chemical-free boundary located 100 m from the center. For the homogeneous aquifer model, the numeric grid consists of 44 elements in the radial direction and 28 elements in the vertical direction. The numeric grid for the heterogeneous aquifer has 42 elements in the radial direction and 31 in the vertical direction. In general, the numeric mesh is finer near the well (0.25 m wide out to a 2 m radius) and within the clay disk (element height is 0.25 m) and becomes progressively coarser farther from the well and in the upper portions of the vadose zone. For example, in the heterogeneous case, the sparging influence is contained within a 20 m radius; at this radius the element width is 1 m. The well bore forms the centerline of the model grid. The sparge gridblock represents a 0.152 m (6 inch) diameter sparge well, screened 0.5 m high, one meter from the bottom. The SVE well screen is a 2 m high gridblock with the bottom placed 1.5 m above the water table. A constant SVE well vacuum pressure of 0.9 atmospheres is specified, which is typical for SVE/air sparging systems (Felten, et al., 1992; Leonard and Brown, 1992). The sparging system is simulated such that the volumetric flow ratio of extracted to injected air is about 6:1 for each case. Wisconsin requires at least a 4:1 ratio (Loden, 1992) to prevent vadose zone vapor migration. Ratios of over 10:1 are also common (Felten et al., 1992; Leonard and Brown, 1992; Loden, 1992).

Porous media parameters such as the intrinsic and relative permeabilities, capillary pressure, and porosity were chosen carefully. For this study, an intrinsic permeability of 10 darcys is used for the homogeneous, sandy medium. A permeability of 10^{-4} darcys is assumed for the clay. The three-phase NAPL permeability is calculated using Stone's first method (Stone, 1970). Parameters which determine the shape of the relative permeability curve are consistent with those given in Mercer and Cohen (1990) for water, TCE, and Xylene in sand and clay. For the three-phase capillary pressure relations, the formulation proposed by Parker et al. (1987) is adopted. The parameters which determine the shape of the capillary pressure for sand were derived from the experimental work of Lenhard and Parker (1987). For the clay, we felt it was important to obtain realistic numbers for breakthrough pressures. The breakthrough pressure is the capillary pressure which must be overcome for the non-wetting fluid (air or NAPL) to enter the largest pores in a water saturated medium. This pressure depends upon the radius of a representative water-filled pore resisting NAPL or air entry, the interfacial tension between the wetting and non-wetting phases, and the contact angles of the fluid-solid interfaces. Realistic values for these parameters were obtained from Mercer and Cohen (1990). Data from van Genuchten (1980) were used to determine the shape of the capillary curves for the clay. For a complete listing of the parameters used in these simulations, the reader is referred to McCray (1994).

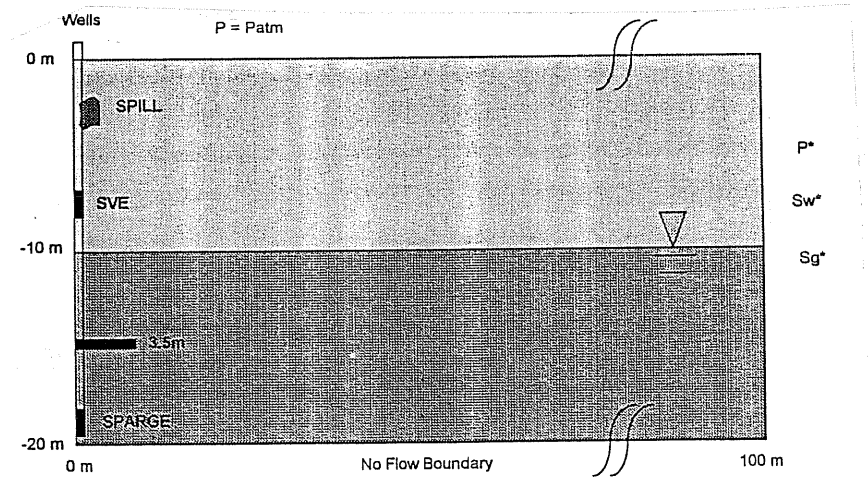

Figure 1. Model aquifer used for air sparging simulations.

Simulation of Sparging in a Homogeneous Medium

For the homogeneous TCE case, 2460 gallons (13602 kg) of liquid TCE is injected at the model grid centerline, 3 meters below the ground surface, at a rate of 50 gallons per day. The spill is allowed to pervade the subsurface for about 1 year prior to initiation of remediation. The initial distribution of TCE NAPL saturation (S_n) is shown in Figure 2a. The equilibrium air injection pressure for this simulation is 35 inches of water above hydrostatic. The volumetric sparge rate (Q_{spg}) is 8.6 scfm, and the volumetric flow for SVE (Q_{sve}) is 54 scfm. Air injection and SVE are begun simultaneously.

Upon the initiation of sparging, the injected gas plume is characterized by a transient period during which the gas plume first expands (causing mounding at the water table), and then collapses to form a steady-state plume. Figure 3 shows the gas plume after 4 hours of sparging and at steady state. At 4 hours, there is over 1 foot of significant mounding (70% water) directly above the sparge point. This mounding is due to a combination of the added air pressure and volume, and to density effects (Wisconsin Dept. of Natural Resources, 1993). Martinson and Linck (1993) observed in field pilot tests that 95% of the initial upwelling dissipated within 1 day. Our simulations also suggest that the mounding is transient. By shortly after 3 days, the plume has reached steady state.

Very little DNAPL is removed during the first several days. After 30 days (Figure 4a), NAPL within the higher gas saturations of the air plume are removed. After 1 year, all the NAPL plume above the air sparge point has been removed (Figure 4b). It is important to note that once the gas plume achieves steady state, the saturated zone DNAPL distribution above the sparge point lies almost entirely within the gas plume (defined by 0.1 gas saturation). Under these conditions, removal of the DNAPL by air sparging is quite effective. It may be very difficult to achieve this geometry in a field situation, however.

These simulations suggest that significant NAPL reduction occurs at relatively low gas saturations of less than 0.1. Previous numerical studies (McCray, 1994) also suggest that dissolved concentrations of TCE can be reduced to virtually zero at gas saturations less than 0.1. Apparently, gas saturation is a good measure of the sparging ROI.

Interestingly, the numerical simulations show that contours of steady-state positive pressure take on the same shape as the steady-state gas saturation profile. Figure 5 shows the positive pressure profile after 4 hours of sparging and at steady state. At steady state, the contour of about 3 inches of water pressure is in roughly the same location as the 0.1 gas saturation contour of Figure 3b. However, during the transient phase, the pressure contours do not resemble the gas saturation distribution. The simulations suggest that measurement of pressure response in monitoring wells below the water table after stabilization of the injected gas plume (as evidenced by the subsidence of water table mounding) may provide the best indication of the ROI.

For a multiphase system, this phenomena is due to capillary pressure effects. Once the gas plume geometry stabilizes, the ground water flow velocities become very small, and mainly consist of small convection currents at the edge of the gas plume (Wisconsin Dept. of Natural Resources, 1993). At this point, the ground water is nearly stagnant. Thus, the gage water pressure (P_w) at any location is equal to the hydrostatic pressure (P_{hyd}). Inside the sparge zone, multiphase conditions are present and the gas pressure is related to the gas-water capillary pressure (P_{cgw}) by

$$P_g = P_w + P_{cgw} \quad (1)$$

Since the ground water is at hydrostatic pressure, we propose that the increase in pressure above hydrostatic pressure (P_{pos}) measured in the sparge zone is a direct result of the capillary pressure between the gas and water phases:

$$P_{cgw} = P_g - P_{hyd} = P_{pos} \quad (2)$$

In the field, this pressure increase is easily measured using monitoring well points (Nyer and Sutherson, 1993). Monitoring points will measure the gas pressure rather than the water pressure or NAPL pressure because of the preferential flow of the nonwetting phase into the monitoring point due to capillary gradients. For a gas-aqueous system, and neglecting capillary pressure hysteresis, the capillary pressure given by (2) directly corresponds to some unique volumetric gas saturation, S_g. Most of the ground water cleanup will occur in the aerated zone (Angell, 1992; Leonard and Brown, 1992; McCray, 1994). Thus, assuming that contaminant cleanup occurs at low gas saturations around 0.1, the

positive pressure that corresponds to this gas saturation on a representative capillary pressure versus gas saturation curve for a field site may be used to define the ROI.

This relation is more complicated for the case where NAPL is present because the gas-water capillary pressure may not be easily measurable under three-phase conditions. In this case, the capillary pressure is not uniquely related to gas saturation but depend on all three phase saturations. Thus, there is no simple analytic expression to relate positive pressure to the ROI. However, Figures 6 and 7 illustrate that the positive pressure contours still mimic the gas saturation contours, even where NAPL is present. Again, positive pressure measurements appear to be a superior method for determination of the sparging ROI and for monitoring the shape of the gas plume. Although not shown here, this was also true for anisotropic systems with various permeability ratios (2:1 to 50:1).

Simulation of Sparging in Heterogeneous Media

For the heterogeneous TCE case, 8266 gallons (45747) kg of liquid TCE was injected at a rate of 50 gallons per day. More chemical was injected than in the homogeneous case to ensure that the DNAPL pooled on the bottom boundary. The TCE spill was allowed to move through the subsurface for nearly 6 months prior to the start of remediation. The initial distribution of NAPL saturation is shown in Figure 2b. The TCE pools on the disk surface since the weight of the DNAPL column is insufficient to overcome the breakthrough pressure.

The injection pressure and flow rates for this scenario are the same as for the homogeneous case. Figure 6 shows the transient and steady-state gas plumes. The clay also acts as a capillary barrier to the injected air for the given injection pressure. Thus, the air collects underneath the lens and eventually travels to the edge where it continues its upward movement.

Figure 7 illustrates the NAPL plume at 30 days and at 1 year (where the steady-state positive pressure distribution is superimposed over the NAPL plume to show its relation to the sparging ROI). Steady state is reached shortly after 3 days for both the gas plume and pressure. As in the homogeneous case, the transient pressure contours do not concur with the gas saturations (not shown), while at steady state, the positive pressure distribution mimics the shape of the gas plume. Note that the gas plume does not significantly contact the DNAPL plume above or below the clay lens except near the edge of the lens. For this reason, no DNAPL is removed directly above the clay. After a year, the vadose zone cleanup of the NAPL phase is complete, but in the saturated zone, only the chemical contained within the ROI is reduced. These simulations suggest that heterogeneities significantly impact sparging performance. Significant cleanup occurs within the injected air plume. Outside the plume, NAPL cleanup will be limited by diffusive and convective transport to the plume. Air sparging could still be effective in remediation for this case if additional wells were used. However, care must be taken in design to prevent migration of vaporous or dissolved contaminant.

Conclusions

Numerical modeling of the air sparging process is possible, even in heterogeneous media, but the distribution of capillarity and permeability must be well known. Gas flow patterns during sparging are strongly affected by heterogeneities, which may result in poor contact between the advective air phase and the pollutant chemical. Thus, sparging efficiency may be significantly degraded where the DNAPL is pooled on relatively impermeable barriers. Multiple sparging wells at various depths may be required to remove significant amounts of DNAPL in these cases.

The ability to make an accurate determination of the radius of cleanup is invaluable since the cost benefits of using air sparging for NAPL and dissolved cleanup will be greatly improved by matching the contaminant plume to this radius. Measurement of the steady-state pressure increase below the water table is recommended as the method of choice for determining the sparging ROI. Positive pressure measurements obtained prior to stabilization of the gas plume are not indicative of the ROI, but rather, reflect in part the transient ground water flow which occurs as the gas plume develops. Based on its transient nature, water table mounding is not a reliable indicator of the sparging radius of influence. The pressure increase present after gas plume steady state is achieved may be directly related to capillary pressure. When no NAPL is present, the ROI may be estimated by comparing the gas-water capillary pressure for a given gas saturation to field-measured positive pressure. When NAPL is present, the positive pressure distribution still mimics the gas saturation profile, and its measurement remains the best method to estimate the ROI.

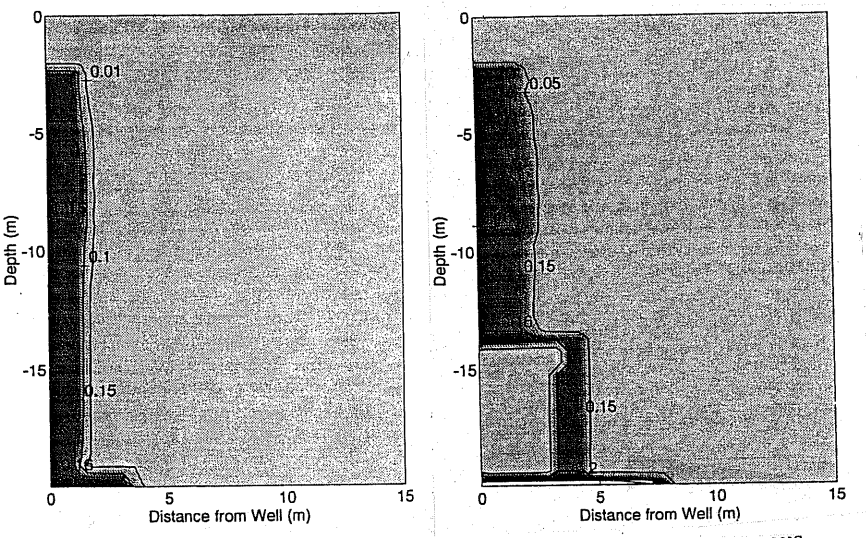

Figure 2. Initial NAPL saturation after the spill in the (a) homogeneous aquifer, and (b) the heterogeneous aquifer.

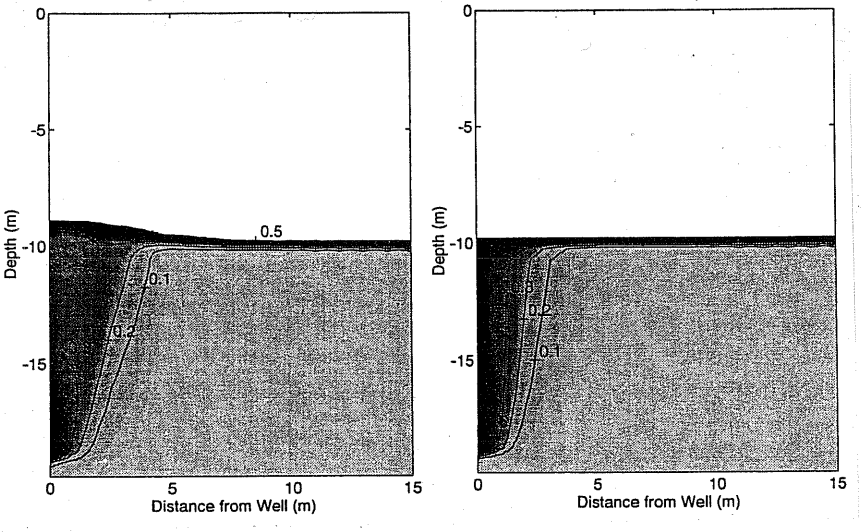

Figure 3. Gas saturation distribution at (a) 4 hours after the initiation of sparging, (b) steady-state in the homogeneous aquifer.

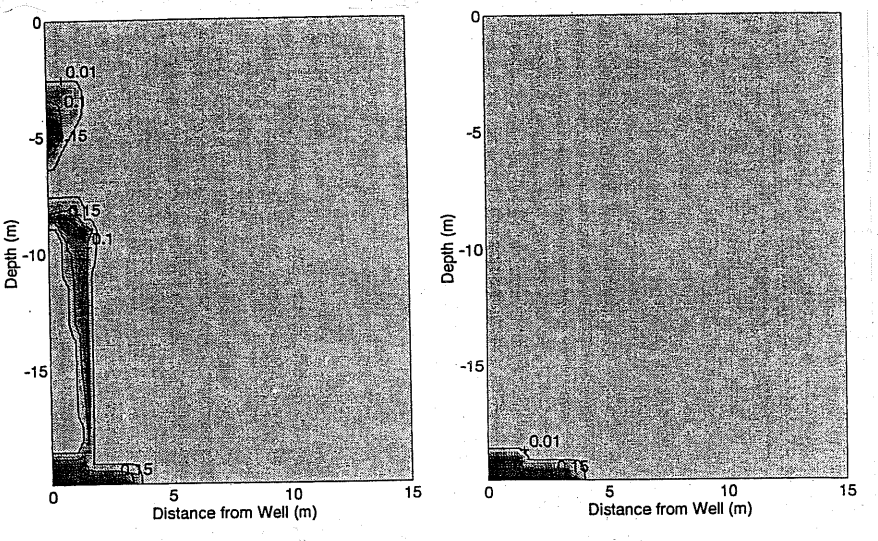

Figure 4. NAPL saturation distribution at (a) 30 days, (b) 1 year after the initation of sparging in the homogeneous aquifer.

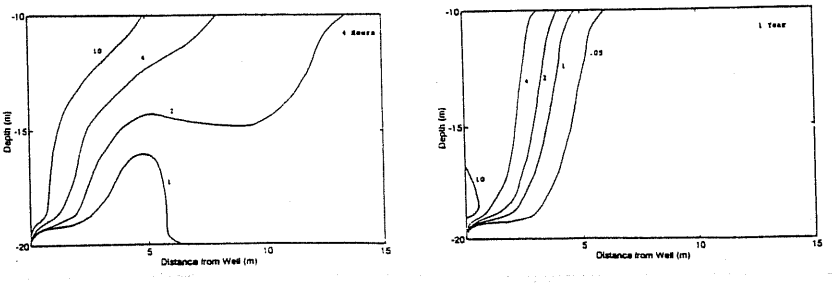

Figure 5. Positive pressure distribution (inches of water) at (a) 4 hours after the initiation of sparging, (b) at steady-state in the homogeneous aquifer.

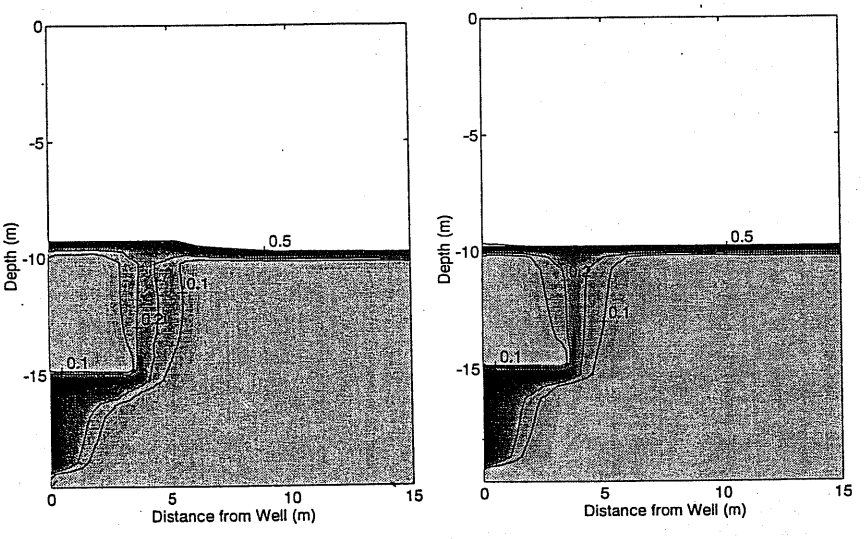

Figure 6. Gas saturation distribution at (a) 4 hours after the initiation of sparging, (b) steady-state in the hetergeneous aquifer.

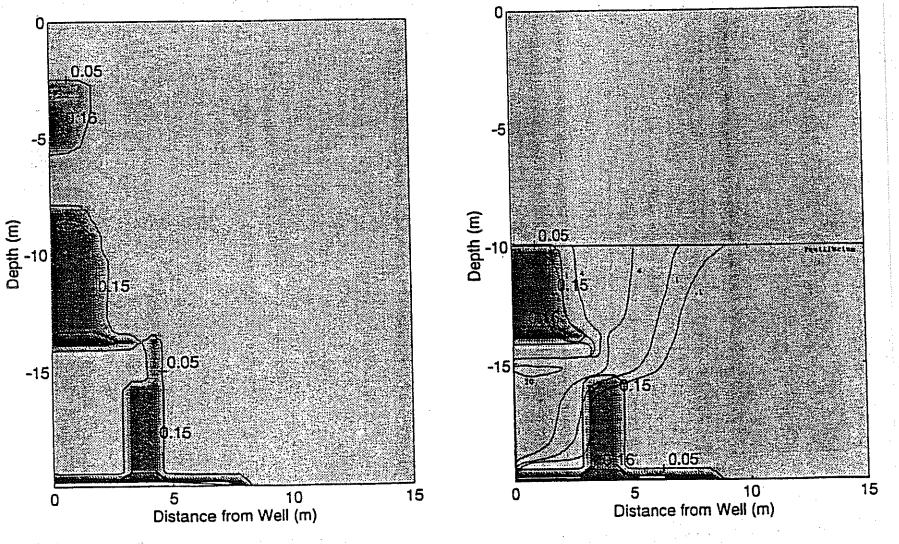

Figure 7. (a) NAPL saturation distribution at 30 days, and (b) at 1 year after the initiation of sparging in the hetergeneous aquifer.

References

Adenekan, A.E., Pruess, K. and Falta, R.W, 1990. Removal of Trichloroethylene contamination from the subsurface: A comparative evaluation of different remediation strategies by means of numerical simulation, Earth Sciences Division Report, Rpt. LBL-30273, Lawrence Berkeley Laboratory, Berkeley.

Angell, K.G., 1992. In situ remedial methods: Air sparging, The National Environmental J., January/February: 20-23.

Falta, R.W., 1990. Multiphase Transport of Organic Contaminants in the Subsurface, Ph.D. Dissertation, University of California at Berkeley, Berkeley.

Falta, R.W. , Pruess, K. Javandel, I., and Witherspoon, P.A., 1992a. Numerical modeling of steam injection for the removal of nonaqueous phase liquids from the subsurface, 1. Numerical formulation, Water Resour. Res., 28(2), 451-465.

Falta, R.W. , Pruess, K. Javandel, I., and Witherspoon, P.A., 1992b. Numerical modeling of steam injection for the removal of nonaqueous phase liquids from the subsurface, 2. Code validation, Water Resour. Res., 28(2): 466-476.

Felten, D.W., Leahy, M.C., Bealer, L.J., and Kline B.A., 1992. Case study: Site remediation using air sparging and soil vapor extraction, in Proceedings of the Petroleum Hydrocarbons and Organic Chemicals in Ground Water: Prevention, Detection, and Restoration Conference, 395-411, National Ground Water Association, Dublin, Ohio.

Ji, W., Dahmani, A., Ahlfeld, D.P., Lin, J.D., Hill, E.,1993. Laboratory study of air sparging: Air flow visualization, Ground Water Monitoring and Remediation, 13(4): 115-127.

Lenhard, R.J. and Parker, J.C., 1987. Measurement and prediction of saturation-pressure relationships in three-phase porous media systems, J. Contaminant Hydrol., 1: 407-424.

Leonard, W.C., and Brown, R.A., 1992. Air sparging: An optimal solution, in Proceedings of the Petroleum Hydrocarbons and Organic Chemicals in Ground Water: Prevention, Detection, and Restoration Conference, 349-363, National Ground Water Association, Dublin, Ohio.

Loden, M. E., 1992. A Technology Assessment of Soil Vapor Extraction and Air Sparging, U.S. EPA/600/R-92/173, U. S. EPA Office of Research and Development, Washington, D.C.

McCray, J.E., 1994. Numerical Analysis of Air Sparging for Subsurface Remediation, Master's. Thesis, Clemson University, Clemson, S.C.

Martinson, M. M., and Linck, J.A, 1993. Field pilot-testing for air sparging of hydrocarbon-contaminated ground water, Proceedings of the Sixteenth International Madison Waste Conference (in print), University of Wisconsin-Madison.

Mercer, J.W. and Cohen, R.M.,1990. A review of immiscible fluids in the subsurface: Properties, models, remediation, and characterization, J. Contaminant Hydrol., 6:107-163.

Nyer, E.K. and Sutherson, S.A. 1993. Air sparging: Savior of groundwater remediations or just blowing bubbles in the bath tub?, Ground Water Monitoring and Remediation 13(4): 87-91.

Parker, J.C., Lenhard, R.J., and Kuppusamy, T., 1987. A parametric model for constitutive properties governing multiphase flow in porous media, Water Resour. Res., 23(4): 618-624.

Pruess, K., 1991. TOUGH2-A general purpose numerical simulator for multiphase fluid and heat flow Rep. LBL-29400, Lawrence Berkeley Laboratory, Berkeley.

Seely, G.E., Falta, R.W., and Hunt, J.R., 1994. Buoyant advection of gases in unsaturated soil, ASCE J. Environmental Engineering, 120 (5).

Stone, H.L., 1970. Probability model for estimating three phase relative permeability, *J. Pet. Technol., 22*(1), 214-218.

van Genuchten, M.T., 1980. A closed form equation for predicting the hydraulic conductivity of unsaturated soils, Soil Sci. Soc. Am. J., 44: 892-898.

Wisconsin Department of Natural Resources, 1993. Guidance for the design, installation, and operation of in situ air sparging systems, Publication PBL-SW186-93.